

## MESHLESS LOCAL PETROV-GALERKIN METHOD FOR MODELING OF SMART STRUCTURES

J. Sladek<sup>1</sup>, V. Sladek<sup>1</sup>, P. Solec<sup>2</sup>, Ch. Zhang<sup>3</sup>

**Summary:** *A meshless method based on the local Petrov-Galerkin approach is proposed, to solve boundary value problems of piezoelectric and magneto-electro-elastic solids with continuously varying material properties. Stationary and transient dynamic 2-D problems are considered in this paper. The mechanical fields are described by the equations of motion with an inertial term. To eliminate the time-dependence in the governing partial differential equations the Laplace-transform technique is applied to the governing equations, which are satisfied in the Laplace-transformed domain in a weak-form on small subdomains. Nodal points are spread on the analyzed domain, and each node is surrounded by a small circle for simplicity. The spatial variation of the displacements as well as the electric and magnetic potentials are approximated by the Moving Least-Squares (MLS) scheme. After performing the spatial integrations, one obtains a system of linear algebraic equations for nodal unknowns.*

### 1. Introduction

Modern smart structures, made of piezoelectric and piezomagnetic materials, offer certain potential performance advantages over conventional ones, due to their capability of converting the energy from one type to other (Berlingcourt et al., 1964; Landau et al., 1984; Nan, 1994). While the piezoelectric and piezomagnetic effects are due to electro-elastic and magneto-elastic interaction, respectively, the magnetoelectric effect is the induction of the electrical polarization by magnetic field and the induction of magnetization by electric field via electro-magneto-elastic interactions. Magnetoelectric coupling plays an important role in the dynamic behaviour of certain materials, especially compounds which possess simultaneously ferroelectric and ferromagnetic phases [Eringen and Maugin, (1990)]. The electric and magnetic symmetry groups for certain crystals permit the piezoelectric and piezomagnetic as well as magnetoelectric effects. In centrosymmetric crystals neither of these effects exists. However, remarkably large magnetoelectric effects are observed for composites than for either composite constituent [Nan, (1994); Feng and Su, (2006)]. If the volume fraction of constituents is varying in a predominant direction then we obtain the so-called functionally graded materials (FGMs). Originally these materials have been introduced to benefit from the ideal performance of its constituents, e.g. high heat and corrosion resistance of ceramics on one side, and large mechanical strength and toughness of metals on the other side. A review on various aspects of FGMs can be found in the monograph of Suresh and Mortensen (1998). Later, the demand

---

<sup>1</sup> Prof. Ing. Jan Sladek, DrSc., Prof. RNDr. Vladimír Sladek, DrSc.: USTARCH SAV, 84503 Bratislava; e-mail: sladek@savba.sk; <sup>2</sup> Doc. Ing. Peter Solec, CSc.: SjF STU, Nam. Slobody 17, Bratislava; <sup>3</sup> Prof. Dr. Chuanzeng Zhang, Civil Engn., University of Siegen, Siegen, Germany

for piezoelectric materials with high strength, high toughness, low thermal expansion coefficient and low dielectric constant encourages the study of functionally graded piezoelectric materials [Zhu et al. (1995); Han et al. (2006)]. According to the best of authors' knowledge there is only one paper [Feng and Su, (2006)] known in literature dealing with continuously nonhomogeneous magneto-electric materials.

The solution of general boundary value problems for continuously nonhomogeneous magneto-electro-elastic solids requires advanced numerical methods due to the high mathematical complexity. Besides this complication, the magnetic, electric and mechanical fields are coupled with each other in the constitutive equations. In spite of the great success of the finite element method (FEM) and boundary element method (BEM) as effective numerical tools for the solution of boundary value problems in elastic solids, there is still a growing interest in the development of new advanced numerical methods. In recent years, meshless formulations are becoming popular due to their high adaptability and low costs to prepare input and output data in numerical analysis. The moving least-squares (MLS) approximation is generally considered as one of many schemes to interpolate discrete data with a reasonable accuracy. A variety of meshless methods has been proposed so far, with some of them being applied only to piezoelectric problems [Ohs and Aluru, (2001); Liu et al., (2002)]. They can be derived from a weak-form formulation either on the global domain or on a set of local subdomains. In the global formulation, background cells are required for the integration of the weak-form. In methods based on local weak-form formulation, no background cells are required and therefore they are often referred to as truly meshless methods. The meshless local Petrov-Galerkin (MLPG) method is a fundamental base for the derivation of many meshless formulations, since trial and test functions can be chosen from different functional spaces (Atluri et al., 2000; Atluri, 2004; Sladek et al., 2000, 2001, 2003). Recently, the MLPG method with a Heaviside step function as the test functions (Atluri et al., 2003; Sladek et al., 2004) has been applied to solve two-dimensional (2-D) homogeneous and continuously nonhomogeneous piezoelectric solids (Sladek et al., 2006, 2007a,b).

In the present paper, the MLPG method is applied to 2-D continuously nonhomogeneous piezoelectric and magneto-electro-elastic solids. The coupled governing partial differential equations are satisfied in a weak form on small fictitious subdomains. Nodal points are introduced and spread on the analyzed domain and each node is surrounded by a small circle for simplicity, but without loss of generality. For a simple shape of subdomains, e.g. circular shape as used in this paper, numerical integrations over them can be easily carried out. The integral equations have a very simple nonsingular form. The spatial variations of the displacements as well as the electric and magnetic potentials are approximated by the moving least-squares scheme (Belytschko et al., 1996; Atluri, (2004)). After performing the spatial integrations, a system of linear algebraic equations for the nodal unknowns is obtained.

## 2. Local boundary integral equations

Basic equations of phenomenological theory of nonconducting elastic materials consist of the governing equations (Maxwell's equations, the balance of momentum) and the constitutive relations. An electro-elastic problem can be considered as a special case of a general magneto-electro-elastic problem. Therefore, a formulation is given here for a general magneto-electro-elastic problem. The governing equations, which are complemented by the boundary and initial conditions, should be solved for the unknown primary field variables such as the elastic displacement vector field  $u_i(\mathbf{x}, \tau)$ , the electric potential  $\psi(\mathbf{x}, \tau)$  (or its gradient, called the

electric vector field  $E_i(\mathbf{x}, \tau)$ , and the magnetic potential  $\mu(\mathbf{x}, \tau)$  (or its gradient, called the magnetic intensity field  $H_i(\mathbf{x}, \tau)$ ). The constitutive equations correlate the primary fields  $\{u_i, E_i, H_i\}$  with the secondary fields  $\{\sigma_{ij}, D_i, B_i\}$  which are the stress tensor field, the electric displacement vector field, and the magnetic induction vector field, respectively. The governing equations give not only the relationships between conjugated fields in each of the pairs  $(\sigma_{ij}, \varepsilon_{ij})$ ,  $(D_i, E_i)$ ,  $(B_i, H_i)$ , but describe also the electro-magneto-elastic interactions in the phenomenological theory of continuous solids.

The electromagnetic fields can be considered as quasi-static [Parton and Kudryavtsev, (1988)]. Then, the Maxwell equations are reduced to two scalar equations

$$D_{j,j}(\mathbf{x}, \tau) = 0, \quad (1)$$

$$B_{j,j}(\mathbf{x}, \tau) = 0, \quad (2)$$

The rest of the vector Maxwell's equations in quasi-static approximation,  $\nabla \times \mathbf{E} = 0$  and  $\nabla \times \mathbf{H} = 0$ , are satisfied identically by an appropriate representation of the fields  $\mathbf{E}(\mathbf{x}, \tau)$  and  $\mathbf{H}(\mathbf{x}, \tau)$  as gradients of scalar electric and magnetic potentials  $\psi(\mathbf{x}, \tau)$  and  $\mu(\mathbf{x}, \tau)$ , respectively,

$$E_j(\mathbf{x}, \tau) = -\psi_{,j}(\mathbf{x}, \tau), \quad (3)$$

$$H_j(\mathbf{x}, \tau) = -\mu_{,j}(\mathbf{x}, \tau). \quad (4)$$

To complete the set of governing equations, eqs. (1) and (2), one needs to use the equations of motion in an elastic continuum

$$\sigma_{ij,j}(\mathbf{x}, \tau) + X_i(\mathbf{x}, \tau) = \rho \ddot{u}_i(\mathbf{x}, \tau), \quad (5)$$

where  $\ddot{u}_i$ ,  $\rho$  and  $X_i$  denote the acceleration of displacements, the mass density, and the body force vector, respectively. A comma after a quantity represents the partial derivatives of the quantity and a dot is used for the time derivative.

Finally, we extend the constitutive equations involving the general electro-magneto-elastic interaction (Nan, 1994) to media with spatially dependent material coefficients for continuously non-homogeneous media

$$\sigma_{ij}(\mathbf{x}, \tau) = c_{ijkl}(\mathbf{x})\varepsilon_{kl}(\mathbf{x}, \tau) - e_{kij}(\mathbf{x})E_k(\mathbf{x}, \tau) - d_{kij}(\mathbf{x})H_k(\mathbf{x}, \tau), \quad (6)$$

$$D_j(\mathbf{x}, \tau) = e_{jkl}(\mathbf{x})\varepsilon_{kl}(\mathbf{x}, \tau) + h_{jk}(\mathbf{x})E_k(\mathbf{x}, \tau) + \alpha_{jk}(\mathbf{x})H_k(\mathbf{x}, \tau), \quad (7)$$

$$B_j(\mathbf{x}, \tau) = d_{jkl}(\mathbf{x})\varepsilon_{kl}(\mathbf{x}, \tau) + \alpha_{kj}(\mathbf{x})E_k(\mathbf{x}, \tau) + \gamma_{jk}(\mathbf{x})H_k(\mathbf{x}, \tau), \quad (8)$$

with the strain tensor  $\varepsilon_{ij}$  being related to the displacements  $u_i$  by

$$\varepsilon_{ij} = \frac{1}{2}(u_{i,j} + u_{j,i}). \quad (9)$$

The functional coefficients  $c_{ijkl}(\mathbf{x})$ ,  $h_{jk}(\mathbf{x})$ , and  $\gamma_{jk}(\mathbf{x})$  are the elastic coefficients, dielectric permittivities, and magnetic permeabilities, respectively;  $e_{kij}(\mathbf{x})$ ,  $d_{kij}(\mathbf{x})$ , and  $\alpha_{jk}(\mathbf{x})$  are the piezoelectric, piezomagnetic, and magnetoelectric coefficients, respectively.

In the case of certain crystal symmetries, one can formulate also the plane-deformation problems (Parton and Kudryavtsev, 1988). For instance, in the crystals of hexagonal symmetry with  $x_3$  being the 6-order symmetry axis and assuming  $u_2 = 0$  as well as the independence on  $x_2$ , i.e.  $(\cdot)_{,2} = 0$ , we have  $\varepsilon_{22} = \varepsilon_{23} = \varepsilon_{12} = E_2 = H_2 = 0$ . Then, the constitutive equations (6) - (8) are reduced to the following form

$$\begin{aligned}
 \begin{bmatrix} \sigma_{11} \\ \sigma_{33} \\ \sigma_{13} \end{bmatrix} &= \begin{bmatrix} c_{11} & c_{13} & 0 \\ c_{13} & c_{33} & 0 \\ 0 & 0 & c_{44} \end{bmatrix} \begin{bmatrix} \varepsilon_{11} \\ \varepsilon_{33} \\ 2\varepsilon_{13} \end{bmatrix} - \begin{bmatrix} 0 & e_{31} \\ 0 & e_{33} \\ e_{15} & 0 \end{bmatrix} \begin{bmatrix} E_1 \\ E_3 \end{bmatrix} - \begin{bmatrix} 0 & d_{31} \\ 0 & d_{33} \\ d_{15} & 0 \end{bmatrix} \begin{bmatrix} H_1 \\ H_3 \end{bmatrix} = \\
 &= \mathbf{C}(\mathbf{x}) \begin{bmatrix} \varepsilon_{11} \\ \varepsilon_{33} \\ 2\varepsilon_{13} \end{bmatrix} - \mathbf{L}(\mathbf{x}) \begin{bmatrix} E_1 \\ E_3 \end{bmatrix} - \mathbf{K}(\mathbf{x}) \begin{bmatrix} H_1 \\ H_3 \end{bmatrix}, \tag{10}
 \end{aligned}$$

$$\begin{aligned}
 \begin{bmatrix} D_1 \\ D_3 \end{bmatrix} &= \begin{bmatrix} 0 & 0 & e_{15} \\ e_{31} & e_{33} & 0 \end{bmatrix} \begin{bmatrix} \varepsilon_{11} \\ \varepsilon_{33} \\ 2\varepsilon_{13} \end{bmatrix} + \begin{bmatrix} h_{11} & 0 \\ 0 & h_{33} \end{bmatrix} \begin{bmatrix} E_1 \\ E_3 \end{bmatrix} + \begin{bmatrix} \alpha_{11} & 0 \\ 0 & \alpha_{33} \end{bmatrix} \begin{bmatrix} H_1 \\ H_3 \end{bmatrix} = \\
 &= \mathbf{G}(\mathbf{x}) \begin{bmatrix} \varepsilon_{11} \\ \varepsilon_{33} \\ 2\varepsilon_{13} \end{bmatrix} + \mathbf{H}(\mathbf{x}) \begin{bmatrix} E_1 \\ E_3 \end{bmatrix} + \mathbf{A}(\mathbf{x}) \begin{bmatrix} H_1 \\ H_3 \end{bmatrix}, \tag{11}
 \end{aligned}$$

$$\begin{aligned}
 \begin{bmatrix} B_1 \\ B_3 \end{bmatrix} &= \begin{bmatrix} 0 & 0 & d_{15} \\ d_{31} & d_{33} & 0 \end{bmatrix} \begin{bmatrix} \varepsilon_{11} \\ \varepsilon_{33} \\ 2\varepsilon_{13} \end{bmatrix} + \begin{bmatrix} \alpha_{11} & 0 \\ 0 & \alpha_{33} \end{bmatrix} \begin{bmatrix} E_1 \\ E_3 \end{bmatrix} + \begin{bmatrix} \gamma_{11} & 0 \\ 0 & \gamma_{33} \end{bmatrix} \begin{bmatrix} H_1 \\ H_3 \end{bmatrix} = \\
 &= \mathbf{R}(\mathbf{x}) \begin{bmatrix} \varepsilon_{11} \\ \varepsilon_{33} \\ 2\varepsilon_{13} \end{bmatrix} + \mathbf{A}(\mathbf{x}) \begin{bmatrix} E_1 \\ E_3 \end{bmatrix} + \mathbf{M}(\mathbf{x}) \begin{bmatrix} H_1 \\ H_3 \end{bmatrix}, \tag{12}
 \end{aligned}$$

Recall that  $\sigma_{22}$  does not influence the governing equations, although it is not vanishing in general, since  $\sigma_{22} = c_{12}\varepsilon_{12} + c_{13}\varepsilon_{33} - e_{13}E_3$ .

The following essential and natural boundary conditions are assumed for the mechanical field

$$\begin{aligned}
 u_i(\mathbf{x}, \tau) &= \tilde{u}_i(\mathbf{x}, \tau), & \text{on } \Gamma_u, \\
 t_i(\mathbf{x}, \tau) &= \sigma_{ij}n_j = \tilde{t}_i(\mathbf{x}, \tau), & \text{on } \Gamma_t, \quad \Gamma = \Gamma_u \cup \Gamma_t.
 \end{aligned}$$

For the electrical field, we assume

$$\begin{aligned}
 \psi(\mathbf{x}, \tau) &= \tilde{\psi}(\mathbf{x}, \tau), & \text{on } \Gamma_p, \\
 n_i(\mathbf{x})D_i(\mathbf{x}, \tau) &\equiv Q(\mathbf{x}, \tau) = \tilde{Q}(\mathbf{x}, \tau), & \text{on } \Gamma_q, \quad \Gamma = \Gamma_p \cup \Gamma_q
 \end{aligned}$$

and for the magnetic field

$$\begin{aligned}
 \mu(\mathbf{x}, \tau) &= \tilde{\mu}(\mathbf{x}, \tau), & \text{on } \Gamma_a, \\
 n_i(\mathbf{x})B_i(\mathbf{x}, \tau) &\equiv S(\mathbf{x}, \tau) = \tilde{S}(\mathbf{x}, \tau), & \text{on } \Gamma_b, \quad \Gamma = \Gamma_a \cup \Gamma_b
 \end{aligned}$$

where  $\Gamma_u$  is the part of the global boundary  $\Gamma$  with prescribed displacements, while on  $\Gamma_t$ ,  $\Gamma_p$ ,  $\Gamma_q$ ,  $\Gamma_a$ , and  $\Gamma_b$  the traction vector, the electric potential, the normal component of the electric displacement vector, the magnetic potential and the magnetic flux are prescribed, respectively. Recall that  $\tilde{Q}(\mathbf{x}, \tau)$  can be considered approximately as the surface density of free charge, provided that the permittivity of the solid is much greater than that of the surrounding medium (vacuum).

The initial conditions for the mechanical displacements are assumed as

$$u_i(\mathbf{x}, \tau)|_{\tau=0} = u_i(\mathbf{x}, 0) \quad \text{and} \quad \dot{u}_i(\mathbf{x}, \tau)|_{\tau=0} = \dot{u}_i(\mathbf{x}, 0) \quad \text{in } \Omega.$$

The Laplace-transform technique is applied to eliminate the time variable in the differential equations. Applying the Laplace-transform to the governing equations (5) one obtains

$$\bar{\sigma}_{ij,j}(\mathbf{x}, p) - \rho(\mathbf{x})p^2\bar{u}_i(\mathbf{x}, p) = -\bar{F}_i(\mathbf{x}, p), \tag{13}$$

where  $p$  is the Laplace-transform parameter and

$$\bar{F}_i(\mathbf{x}, p) = \bar{X}_i(\mathbf{x}, p) + pu_i(\mathbf{x}, 0) + \dot{u}_i(\mathbf{x}, 0),$$

is the re-defined body force in the Laplace-transformed domain with the initial boundary conditions for the displacements  $u_i(\mathbf{x}, 0)$  and velocities  $\dot{u}_i(\mathbf{x}, 0)$ . Recall that the subscripts take now values 1 and 3.

Instead of writing the global weak-form for the above governing equations, the MLPG method constructs a weak-form over the local fictitious subdomains such as  $\Omega_s$ , which is a small region constructed for each node inside the global domain (Atluri, 2004). The local subdomains overlap each other, and cover the whole global domain  $\Omega$ . The local subdomains could be of any geometrical shape and size. In the present paper, the local subdomains are taken to be of a circular shape for simplicity. The local weak-form of the governing equation (13) can be written as

$$\int_{\Omega_s} \left[ \bar{\sigma}_{ij,j}(\mathbf{x}, p) - \rho(\mathbf{x})p^2\bar{u}_i(\mathbf{x}, p) + \bar{F}_i(\mathbf{x}, p) \right] u_{ik}^*(\mathbf{x}) d\Omega = 0, \tag{14}$$

where  $u_{ik}^*(\mathbf{x})$  is a test function.

Applying the Gauss divergence theorem to eq. (14) one obtains

$$\int_{\partial\Omega_s} \bar{\sigma}_{ij}(\mathbf{x}, p)n_j(\mathbf{x})u_{ik}^*(\mathbf{x})d\Gamma - \int_{\Omega_s} \bar{\sigma}_{ij}(\mathbf{x}, p)u_{ik,j}^*(\mathbf{x})d\Omega + \int_{\Omega_s} \left[ \bar{F}_i(\mathbf{x}, p) - \rho(\mathbf{x})p^2\bar{u}_i(\mathbf{x}, p) \right] u_{ik}^*(\mathbf{x})d\Omega = 0, \tag{15}$$

where  $\partial\Omega_s$  is the boundary of the local subdomain which consists of three parts  $\partial\Omega_s = L_s \cup \Gamma_{st} \cup \Gamma_{su}$  (Atluri, 2004) in general. Here,  $L_s$  is the local boundary that is totally inside the global domain,  $\Gamma_{st}$  is the part of the local boundary which coincides with the global traction boundary, i.e.,  $\Gamma_{st} = \partial\Omega_s \cap \Gamma_t$ , and similarly  $\Gamma_{su}$  is the part of the local boundary that coincides with the global displacement boundary, i.e.,  $\Gamma_{su} = \partial\Omega_s \cap \Gamma_u$ .

By choosing a Heaviside step function as the test function  $u_{ik}^*(\mathbf{x})$  in each subdomain as

$$u_{ik}^*(\mathbf{x}) = \begin{cases} \delta_{ik} & \text{at } \mathbf{x} \in \Omega_s \\ 0 & \text{at } \mathbf{x} \notin \Omega_s \end{cases},$$

the local weak-form (15) is converted into the following local boundary-domain integral equations

$$\int_{L_s + \Gamma_{su}} \bar{t}_i(\mathbf{x}, p) d\Gamma - \int_{\Omega_s} \rho(\mathbf{x}) p^2 \bar{u}_i(\mathbf{x}, p) d\Omega = - \int_{\Gamma_{st}} \tilde{t}_i(\mathbf{x}, p) d\Gamma - \int_{\Omega_s} \bar{F}_i(\mathbf{x}, p) d\Omega. \quad (16)$$

Equation (16) is recognized as the overall force equilibrium conditions on the subdomain  $\Omega_s$ . Note that the local integral equations (16) are valid for both the homogeneous and nonhomogeneous solids. Nonhomogeneous material properties are included in eq. (16) through the elastic, piezoelectric and piezomagnetic coefficients in the traction components.

Similarly, the local weak-form of the governing equation (2) can be written as

$$\int_{\Omega_s} \bar{D}_{j,j}(\mathbf{x}, p) v^*(\mathbf{x}) d\Omega = 0, \quad (17)$$

where  $v^*(\mathbf{x})$  is a test function.

Applying the Gauss divergence theorem to the local weak-form (17) and choosing the Heaviside step function as the test function  $v^*(\mathbf{x})$  one can obtain

$$\int_{L_s + \Gamma_{sp}} \bar{Q}(\mathbf{x}, p) d\Gamma = - \int_{\Gamma_{sq}} \bar{Q}(\mathbf{x}, p) d\Gamma, \quad (18)$$

where

$$\bar{Q}(\mathbf{x}, p) = \bar{D}_j(\mathbf{x}, p) n_j(\mathbf{x}) = [e_{jkl} \bar{u}_{k,l}(\mathbf{x}, p) - h_{jk} \bar{\psi}_{,k}(\mathbf{x}, p) - \alpha_{jk} \bar{\mu}_{,k}(\mathbf{x}, p)] n_j.$$

The local integral equation corresponding to the third governing equation (3) has the form

$$\int_{L_s + \Gamma_{sa}} \bar{S}(\mathbf{x}, p) d\Gamma = - \int_{\Gamma_{sb}} \bar{S}(\mathbf{x}, p) d\Gamma, \quad (19)$$

where the magnetic flux is given by

$$\bar{S}(\mathbf{x}, p) = \bar{B}_j(\mathbf{x}, p) n_j(\mathbf{x}) = [d_{jkl} \bar{u}_{k,l}(\mathbf{x}, p) - \alpha_{kj} \bar{\psi}_{,k}(\mathbf{x}, p) - \gamma_{jk} \bar{\mu}_{,k}(\mathbf{x}, p)] n_j.$$

In the MLPG method the test and the trial functions are not necessarily from the same functional spaces. On each local subdomain, the test function is chosen as a unit step function with its support being identical with the local subdomain. The trial functions, on the other hand, are chosen to be the MLS approximations by using a number of nodes spread over the domain of influence. According to the MLS (Belytschko et al., 1996) method, the approximation of the displacements can be given as

$$\mathbf{u}^h(\mathbf{x}) = \sum_{i=1}^m p_i(\mathbf{x}) a_i(\mathbf{x}) = \mathbf{p}^T(\mathbf{x}) \mathbf{a}(\mathbf{x}),$$

where  $\mathbf{p}^T(\mathbf{x}) = \{p_1(\mathbf{x}), p_2(\mathbf{x}), \dots, p_m(\mathbf{x})\}$  is a vector of complete basis functions of order  $m$  and  $\mathbf{a}(\mathbf{x}) = \{a_1(\mathbf{x}), a_2(\mathbf{x}), \dots, a_m(\mathbf{x})\}$  is a vector of unknown parameters that depend on  $\mathbf{x}$ .

The approximated functions for the Laplace-transforms of the mechanical displacements, the electric and magnetic potentials can be written as (Atluri, 2004)

$$\bar{\mathbf{u}}^h(\mathbf{x}, p) = \mathbf{\Phi}^T(\mathbf{x}) \cdot \hat{\mathbf{u}} = \sum_{a=1}^n \phi^a(\mathbf{x}) \hat{\mathbf{u}}^a(p),$$

$$\bar{\psi}^h(\mathbf{x}, p) = \sum_{a=1}^n \phi^a(\mathbf{x}) \hat{\psi}^a(p),$$

$$\bar{\mu}^h(\mathbf{x}, p) = \sum_{a=1}^n \phi^a(\mathbf{x}) \hat{\mu}^a(p), \quad (20)$$

where the nodal values  $\hat{\mathbf{u}}^a(p) = (\hat{u}_1^a(p), \hat{u}_3^a(p))^T$ ,  $\hat{\psi}^a(p)$  and  $\hat{\mu}^a(p)$  are fictitious parameters for the Laplace-transforms of the displacements, the electric and magnetic potentials, respectively, and  $\phi^a(\mathbf{x})$  is the shape function associated with the node  $a$ . The number of nodes  $n$  used for the approximation is determined by the weight function  $w^a(\mathbf{x})$ . A 4<sup>th</sup> order spline-type weight function is applied in the present work

$$w^a(\mathbf{x}) = \begin{cases} 1 - 6\left(\frac{d^a}{r^a}\right)^2 + 8\left(\frac{d^a}{r^a}\right)^3 - 3\left(\frac{d^a}{r^a}\right)^4, & 0 \leq d^a \leq r^a \\ 0, & d^a \geq r^a \end{cases}, \quad (21)$$

where  $d^a = \|\mathbf{x} - \mathbf{x}^a\|$  and  $r^a$  is the size of the support domain. It is seen that the  $C^1$ -continuity is ensured over the entire domain, and therefore the continuity conditions of the tractions, the electric charge and the magnetic flux are satisfied.

The Laplace-transform of the traction vector  $\bar{t}_i(\mathbf{x}, p)$  at a boundary point  $\mathbf{x} \in \partial\Omega_s$  is approximated in terms of the same nodal values  $\hat{\mathbf{u}}^a(p)$  as

$$\bar{\mathbf{t}}^h(\mathbf{x}, p) = \mathbf{N}(\mathbf{x})\mathbf{C}(\mathbf{x}) \sum_{a=1}^n \mathbf{B}^a(\mathbf{x}) \hat{\mathbf{u}}^a(p) + \mathbf{N}(\mathbf{x})\mathbf{L}(\mathbf{x}) \sum_{a=1}^n \mathbf{P}^a(\mathbf{x}) \hat{\psi}^a(p) + \mathbf{N}(\mathbf{x})\mathbf{K}(\mathbf{x}) \sum_{a=1}^n \mathbf{P}^a(\mathbf{x}) \hat{\mu}^a(p), \quad (22)$$

where the matrices  $\mathbf{C}(\mathbf{x})$ ,  $\mathbf{L}(\mathbf{x})$  and  $\mathbf{K}(\mathbf{x})$  are defined in eq. (10), the matrix  $\mathbf{N}(\mathbf{x})$  is related to the normal vector  $\mathbf{n}(\mathbf{x})$  on  $\partial\Omega_s$  by

$$\mathbf{N}(\mathbf{x}) = \begin{bmatrix} n_1 & 0 & n_3 \\ 0 & n_3 & n_1 \end{bmatrix}$$

and finally, the matrices  $\mathbf{B}^a$  and  $\mathbf{P}^a$  are represented by the gradients of the shape functions as

$$\mathbf{B}^a(\mathbf{x}) = \begin{bmatrix} \phi_{,1}^a & 0 \\ 0 & \phi_{,3}^a \\ \phi_{,3}^a & \phi_{,1}^a \end{bmatrix}, \quad \mathbf{P}^a(\mathbf{x}) = \begin{bmatrix} \phi_{,1}^a \\ \phi_{,3}^a \end{bmatrix}.$$

Similarly the Laplace-transform of the normal component of the electric displacement vector  $\bar{Q}(\mathbf{x}, p)$  can be approximated by

$$\bar{Q}^h(\mathbf{x}, p) = \mathbf{N}_1(\mathbf{x})\mathbf{G}(\mathbf{x}) \sum_{a=1}^n \mathbf{B}^a(\mathbf{x}) \hat{\mathbf{u}}^a(p) - \mathbf{N}_1(\mathbf{x})\mathbf{H}(\mathbf{x}) \sum_{a=1}^n \mathbf{P}^a(\mathbf{x}) \hat{\psi}^a(p) - \mathbf{N}_1(\mathbf{x})\mathbf{A}(\mathbf{x}) \sum_{a=1}^n \mathbf{P}^a(\mathbf{x}) \hat{\mu}^a(p), \quad (23)$$

where the matrices  $\mathbf{G}(\mathbf{x})$ ,  $\mathbf{H}(\mathbf{x})$  and  $\mathbf{A}(\mathbf{x})$  are defined in eq. (11) and

$$\mathbf{N}_1(\mathbf{x}) = [n_1 \quad n_3].$$

Eventually, the Laplace-transform of the magnetic flux  $\bar{S}(\mathbf{x}, p)$  is approximated by

$$\bar{S}^h(\mathbf{x}, p) = \mathbf{N}_1(\mathbf{x})\mathbf{R}(\mathbf{x}) \sum_{a=1}^n \mathbf{B}^a(\mathbf{x}) \hat{\mathbf{u}}^a(p) - \mathbf{N}_1(\mathbf{x})\mathbf{A}(\mathbf{x}) \sum_{a=1}^n \mathbf{P}^a(\mathbf{x}) \hat{\psi}^a(p) - \mathbf{N}_1(\mathbf{x})\mathbf{M}(\mathbf{x}) \sum_{a=1}^n \mathbf{P}^a(\mathbf{x}) \hat{\mu}^a(p). \quad (24)$$

Satisfying the essential boundary conditions and making use of the approximation formula (20), one obtains the discretized form of these boundary conditions as

$$\begin{aligned} \sum_{a=1}^n \phi^a(\zeta) \hat{\mathbf{u}}^a(p) &= \bar{\mathbf{u}}(\zeta, p) \quad \text{for } \zeta \in \Gamma_u, \\ \sum_{a=1}^n \phi^a(\zeta) \hat{\psi}^a(p) &= \bar{\psi}(\zeta, p) \quad \text{for } \zeta \in \Gamma_p, \\ \sum_{a=1}^n \phi^a(\zeta) \hat{\mu}^a &= \bar{\mu}(\zeta, p) \quad \text{for } \zeta \in \Gamma_a. \end{aligned} \quad (25)$$

Furthermore, in view of the MLS-approximation (22)-(24) for the unknown quantities in the local boundary-domain integral equations (16), (18) and (19), we obtain their discretized forms as

$$\begin{aligned} \sum_{a=1}^n \left( \int_{L_s + \Gamma_{st}} \mathbf{N}(\mathbf{x}) \mathbf{C}(\mathbf{x}) \mathbf{B}^a(\mathbf{x}) d\Gamma - \mathbf{I} \rho p^2 \int_{\Omega_s} \phi^a(\mathbf{x}) d\Omega \right) \hat{\mathbf{u}}^a(p) + \sum_{a=1}^n \left( \int_{L_s + \Gamma_{sq}} \mathbf{N}(\mathbf{x}) \mathbf{L}(\mathbf{x}) \mathbf{P}^a(\mathbf{x}) d\Gamma \right) \hat{\psi}^a(p) + \\ + \sum_{a=1}^n \left( \int_{L_s + \Gamma_{sb}} \mathbf{N}(\mathbf{x}) \mathbf{K}(\mathbf{x}) \mathbf{P}^a(\mathbf{x}) d\Gamma \right) \hat{\mu}^a(p) = - \int_{\Gamma_{st}} \bar{\mathbf{t}}(\mathbf{x}, p) d\Gamma - \int_{\Omega_s} \bar{\mathbf{F}}(\mathbf{x}, p) d\Omega, \end{aligned} \quad (26)$$

$$\begin{aligned} \sum_{a=1}^n \left( \int_{L_s + \Gamma_{sp}} \mathbf{N}_1(\mathbf{x}) \mathbf{G}(\mathbf{x}) \mathbf{B}^a(\mathbf{x}) d\Gamma \right) \hat{\mathbf{u}}^a(p) - \sum_{a=1}^n \left( \int_{L_s + \Gamma_{sp}} \mathbf{N}_1(\mathbf{x}) \mathbf{H}(\mathbf{x}) \mathbf{P}^a(\mathbf{x}) d\Gamma \right) \hat{\psi}^a(p) - \\ - \sum_{a=1}^n \left( \int_{L_s + \Gamma_{sp}} \mathbf{N}_1(\mathbf{x}) \mathbf{A}(\mathbf{x}) \mathbf{P}^a(\mathbf{x}) d\Gamma \right) \hat{\mu}^a(p) = - \int_{\Gamma_{sq}} \bar{\mathbf{Q}}(\mathbf{x}, p) d\Gamma, \end{aligned} \quad (27)$$

$$\begin{aligned} \sum_{a=1}^n \left( \int_{L_s + \Gamma_{sp}} \mathbf{N}_1(\mathbf{x}) \mathbf{R}(\mathbf{x}) \mathbf{B}^a(\mathbf{x}) d\Gamma \right) \hat{\mathbf{u}}^a(p) - \sum_{a=1}^n \left( \int_{L_s + \Gamma_{sp}} \mathbf{N}_1(\mathbf{x}) \mathbf{A}(\mathbf{x}) \mathbf{P}^a(\mathbf{x}) d\Gamma \right) \hat{\psi}^a(p) - \\ - \sum_{a=1}^n \left( \int_{L_s + \Gamma_{sp}} \mathbf{N}_1(\mathbf{x}) \mathbf{M}(\mathbf{x}) \mathbf{P}^a(\mathbf{x}) d\Gamma \right) \hat{\mu}^a(p) = - \int_{\Gamma_{sq}} \bar{\mathbf{S}}(\mathbf{x}, p) d\Gamma, \end{aligned} \quad (28)$$

which are considered on the sub-domains adjacent to the interior nodes as well as to the boundary nodes on  $\Gamma_{st}$ ,  $\Gamma_{sq}$  and  $\Gamma_{sb}$  and  $\mathbf{I}$  is a unit matrix.

Collecting the discretized local boundary-domain integral equations together with the discretized boundary conditions for essential boundary conditions results in the complete system of linear algebraic equations for the computation of the nodal unknowns, namely, the Laplace-transforms of the fictitious parameters  $\hat{\mathbf{u}}^a(p)$ ,  $\hat{\psi}^a(p)$  and  $\hat{\mu}^a(p)$ . The time dependent values of the transformed quantities can be obtained by an inverse Laplace-transform. In the present analysis, the Stehfest's inversion algorithm (Stehfest, 1970) is used.

### 3. Numerical examples

In the first example, numerical results for the bending of a square piezoelectric panel are presented to illustrate the accuracy of the proposed method. The square panel with a size



$a \times a = 1\text{mm} \times 1\text{mm}$  made of a PZT-4 material is subjected to a pure bending moment arising from a linearly varying stress at the right boundary (Fig. 1). The lower boundary of the panel is earthed, i.e. vanishing electrical potential is assumed on this side of panel. The other boundaries have prescribed vanishing electrical charge.

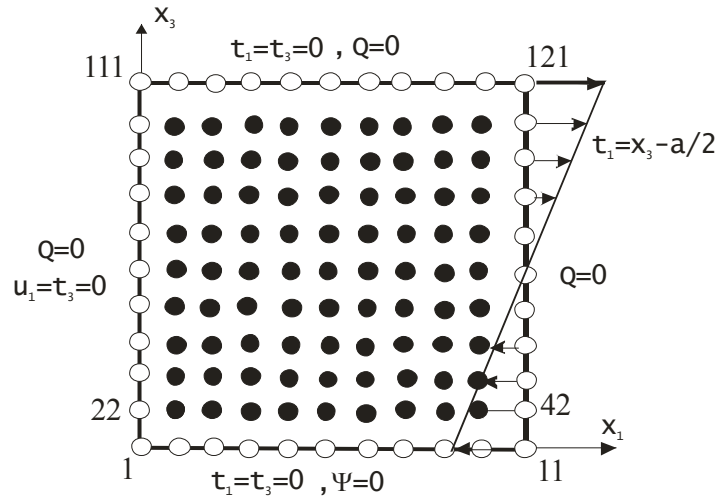


Fig. 1 Bending of a square piezoelectric panel

The material coefficients corresponding to PZT-4 are following

$$\begin{aligned}
 c_{11} &= 13.9 \cdot 10^{10} \text{ Nm}^{-2}, & c_{13} &= 7.43 \cdot 10^{10} \text{ Nm}^{-2}, & c_{33} &= 11.3 \cdot 10^{10} \text{ Nm}^{-2}, \\
 c_{44} &= 2.56 \cdot 10^{10} \text{ Nm}^{-2}, & e_{15} &= 13.44 \text{ Cm}^{-2}, & e_{31} &= -6.98 \text{ Cm}^{-2}, & e_{33} &= 13.84 \text{ Cm}^{-2}, \\
 h_{11} &= 6.0 \cdot 10^{-9} \text{ C(Vm)}^{-1}, & h_{33} &= 5.47 \cdot 10^{-9} \text{ C(Vm)}^{-1}.
 \end{aligned}$$

The mechanical displacement and the electrical potential fields on the finite square panel are approximated by using 121 (11x11) nodes equidistantly distributed. First, a static loading condition is considered.

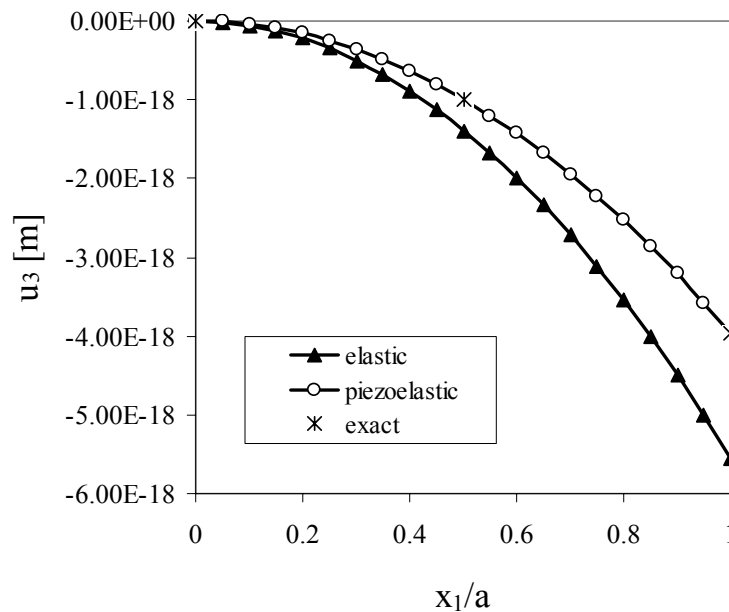


Fig. 2 Variation of the mechanical displacement  $u_3$  with normalized coordinate  $x_1 / a$

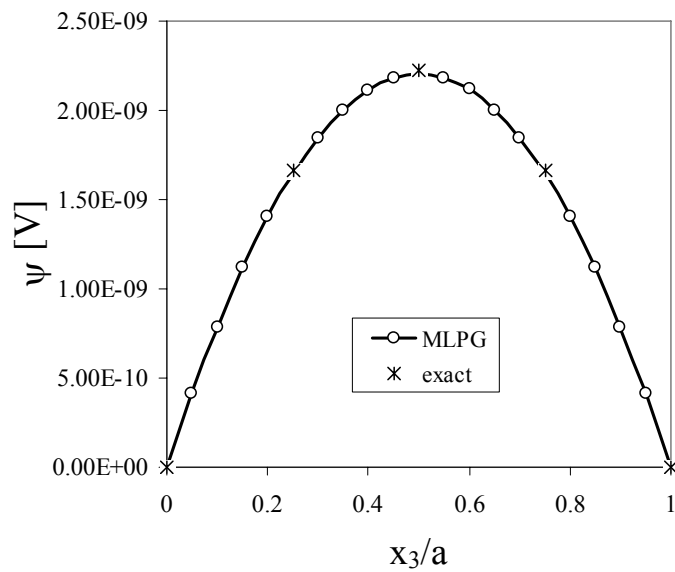


Fig. 3 Variation of the electrical potential with normalized coordinate  $x_3/a$

The analytical solution of the problem is given by Parton et al. (1989). Numerical results for the displacement component  $u_3$  along the line  $x_3 = a/2$  and the electric potential along the line  $x_1 = a/2$  are presented in Figs. 2 and 3. One can observe an excellent agreement of the present results and the exact solution in the whole interval considered. To see the influence of the electrical field on the mechanical displacements the results for a pure elastic panel (without electro-elastic interaction  $e_{15} = e_{31} = e_{33} = 0$ ) are given in Fig. 2 too. For the considered boundary conditions, the mechanical displacement component  $u_3$  is reduced in the piezoelectric panel compared to a pure elastic one.

An edge crack in a finite strip is analyzed in the next example. The sample geometry is given in Fig. 4 with following values:  $a = 0.5$ ,  $a/w = 0.4$  and  $h/w = 1.2$ . Due to the symmetry with respect to  $x_1$  only a half of the specimen is modeled.

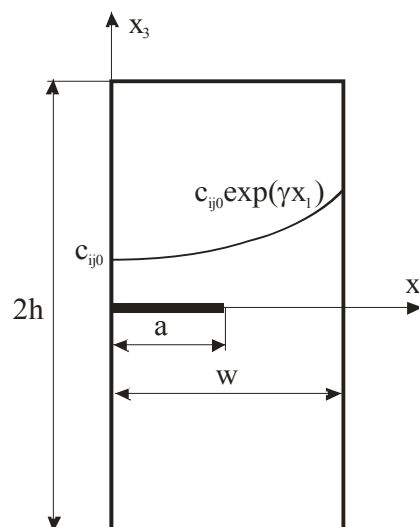


Fig. 4 An edge crack in a finite strip with graded material properties in  $x_1$

We have used 930 nodes equidistantly distributed for the MLS approximation of the physical fields. On the top of the strip a uniform impact tension  $\sigma_0$  and electrical displacement  $D_0$  (Heaviside time variation) are applied, respectively. Impermeable electrical boundary conditions on crack-faces are assumed here (the electrical displacement is vanishing on the crack-faces). Functionally graded material properties in  $x_1$  coordinate are considered. An exponential variation for the elastic, piezoelectric and dielectric tensors is used

$$\begin{aligned} c_{ijkl}(\mathbf{x}) &= c_{ijkl0} \exp(\gamma x_1), \\ e_{ijk}(\mathbf{x}) &= e_{ijk0} \exp(\gamma x_1), \\ h_{ij}(\mathbf{x}) &= h_{ij0} \exp(\gamma x_1), \end{aligned} \quad (31)$$

where  $c_{ijkl0}$ ,  $e_{ijk0}$  and  $h_{ij0}$  correspond to parameters used in the previous example. For cracks in homogeneous and linear piezoelectric and piezomagnetic solids the asymptotic behaviour of the field quantities has been given by Wang and Mai (2003). In the crack-tip vicinity, the displacements and potentials show the classical  $\sqrt{r}$  asymptotic behaviour. Hence, correspondingly, the stresses, the electrical displacement and the magnetic induction exhibit a  $1/\sqrt{r}$  behaviour, where  $r$  is the radial polar coordinate with the origin at the crack-tip. Garcia-Sanchez et al. (2007) extended the approach used in piezoelectricity to magnetoelastoelectricity to obtain the asymptotic expression of generalized intensity factors

$$\begin{pmatrix} K_{II} \\ K_I \\ K_E \\ K_M \end{pmatrix} = \sqrt{\frac{\pi}{2r}} [\text{Re}(\mathbf{B})^{-1}] \begin{pmatrix} u_1 \\ u_3 \\ \psi \\ \mu \end{pmatrix} \quad (32)$$

where the matrix  $\mathbf{B}$  is determined by the material properties (Garcia-Sanchez et al., 2007; Garcia-Sanchez and Saez, 2005) and

$$\begin{aligned} K_I &= \lim_{r \rightarrow 0} \sqrt{2\pi r} \sigma_{33}(r, 0), \\ K_{II} &= \lim_{r \rightarrow 0} \sqrt{2\pi r} \sigma_{13}(r, 0), \\ K_E &= \lim_{r \rightarrow 0} \sqrt{2\pi r} D_3(r, 0), \\ K_M &= \lim_{r \rightarrow 0} \sqrt{2\pi r} B_3(r, 0), \end{aligned}$$

are the stress intensity factors (SIF)  $K_I$  and  $K_{II}$ ,  $K_E$  is the electrical displacement intensity factor (EDIF), and  $K_M$  is the magnetic induction intensity factor (MIIF), respectively.

The influence of the material gradation on the stress intensity factor and the electrical displacement intensity factor is analyzed. The temporal variation of the SIF and the EDIF in the cracked strip under a pure mechanical load is presented in Figs. 5 and 6, respectively. The static stress intensity factor for the considered load and geometry is equal to  $K_I^{stat} = 2.642 \text{ Pa m}^{1/2}$ . Numerical results for a homogeneous strip are compared with the FEM ones, and a quite good agreement is observed. For a gradation of the mechanical material properties with  $x_1$  coordinate and a uniform mass density, the wave propagation is increasing with  $x_1$ . Therefore, the peak value of the SIF is reached in a shorter time instant in FGPM

strip than in a homogeneous one. The maximum value of the SIF is only slightly reduced for the cracked FGPM strip.

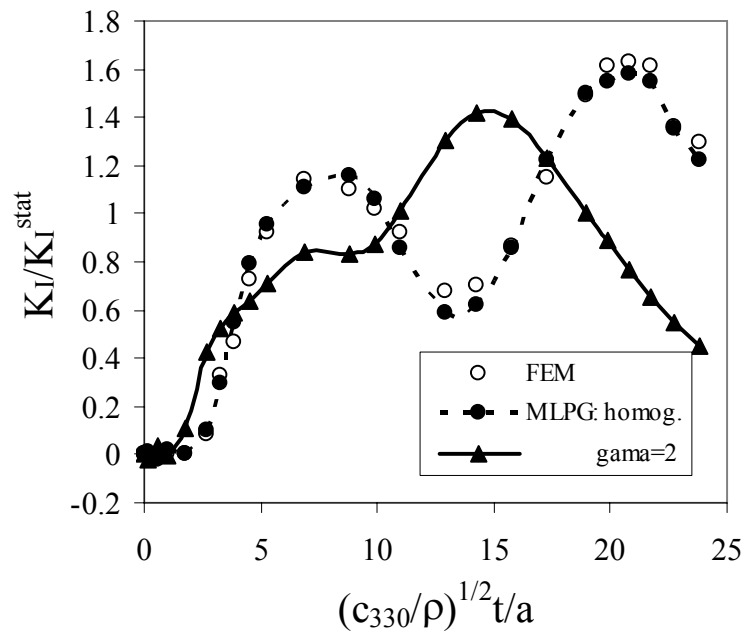


Fig. 5 Influence of the material gradation on the stress intensity factor in a cracked strip under a pure mechanical impact load  $\sigma_0 H(t-0)$

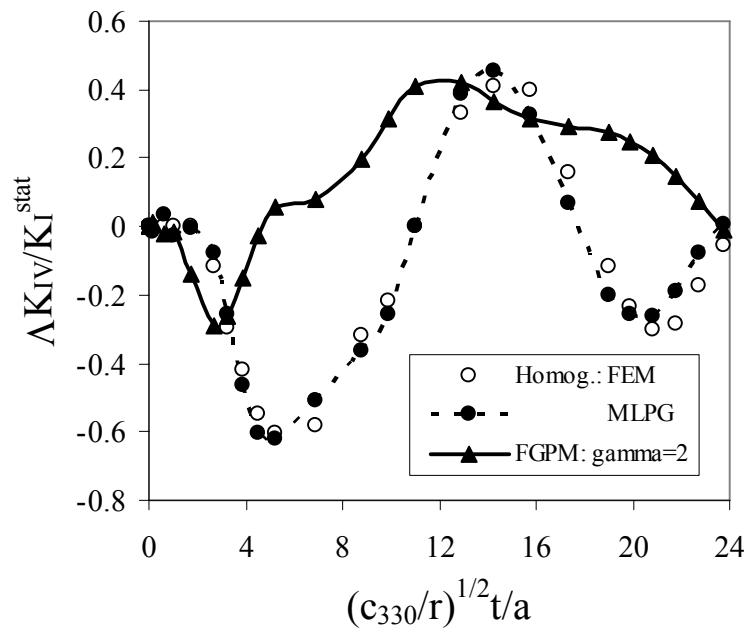


Fig. 6 Influence of the material gradation on the EDIF in a cracked strip under a pure mechanical impact load  $\sigma_0 H(t-0)$

Finally, an edge crack in a finite magneto-electro-elastic strip is analyzed. The geometry of the cracked specimen is the same as in the previous example. We have used again 930 equidistantly distributed nodes for the MLS approximation of the physical fields. On the top of the

strip either a uniform tension  $\sigma_0$  or a uniform magnetic induction  $B_0$  is applied. The functionally graded material properties in the  $x_1$ -direction are considered. An exponential variation of the elastic, piezoelectric, dielectric, paramagnetic, electromagnetic and magnetic permeability coefficients are assumed as

$$f_{ij}(\mathbf{x}) = f_{ij0} \exp(\gamma_f x_1), \quad (32)$$

where the symbol  $f_{ij}$  is used for particular material coefficients with  $f_{ij0}$  corresponding to the material coefficients for the BaTiO<sub>3</sub>-CoFe<sub>2</sub>O<sub>4</sub> composite and being given by Li (2000) as

$$\begin{aligned} c_{11} &= 22.6 \times 10^{10} \text{ Nm}^{-2}, & c_{13} &= 12.4 \times 10^{10} \text{ Nm}^{-2}, & c_{33} &= 21.6 \times 10^{10} \text{ Nm}^{-2}, \\ c_{66} &= 4.4 \times 10^{10} \text{ Nm}^{-2}, & e_{15} &= 5.8 \text{ Cm}^{-2}, & e_{31} &= -2.2 \text{ Cm}^{-2}, & e_{33} &= 9.3 \text{ Cm}^{-2}, \\ h_{11} &= 5.64 \times 10^{-9} \text{ C}^2 / \text{Nm}^2, & h_{33} &= 6.35 \times 10^{-9} \text{ C}^2 / \text{Nm}^2, \\ d_{15} &= 275.0 \text{ N / Am}, & d_{21} &= 290.2 \text{ N / Am}, & d_{22} &= 350.0 \text{ N / Am}, \\ \alpha_{11} &= 5.367 \times 10^{-12} \text{ Ns / VC}, & \alpha_{33} &= 2737.5 \times 10^{-12} \text{ Ns / VC}, \\ \gamma_{11} &= 297.0 \times 10^{-6} \text{ Ns}^2 \text{ C}^{-2}, & \gamma_{33} &= 83.5 \times 10^{-6} \text{ Ns}^2 \text{ C}^{-2}, & \rho &= 5500 \text{ kg / m}^3, \end{aligned}$$

and the origin  $x_1 = 0$  is assumed at the crack-tip.

We have considered the same exponential gradation for all coefficients with the value  $\gamma = 2$  in the numerical calculations. Then, all material parameters at the crack-tip are  $e^1 = 2.718$  times larger than that in the homogeneous material. Then, the crack-opening-displacement and potentials are significantly reduced in the nonhomogeneous material with gradually increasing material properties in  $x_1$ -direction. The normalized stress intensity factors for homogeneous and nonhomogeneous cracked specimen have the following values,  $f_I = K_I / \sigma_0 \sqrt{\pi a} = 2.105$  and 1.565, respectively, for a static load. With increasing gradient parameter  $\gamma$  the SIF is decreasing. A similar phenomenon is observed for an edge crack in an elastic FGM strip under a mechanical loading (Dolbow and Gosz, 2002) and for a cracked piezoelectric FGM specimen (Sladek et al., 2007a). For a crack in a homogeneous magneto-electro-elastic solid the SIF, EDIF and magnetic induction intensity factor (MIIF) are uncoupled. However, this conclusion is not valid generally for a continuously nonhomogeneous solid. We have obtained the following normalized quantities:  $\Lambda_e K_E / K_I^{stat} = 0.04866$  and  $\Lambda_m K_M / K_I^{stat} = 0.00412$ . For normalized electrical displacement and magnetic induction intensity factors we have used the parameters  $\Lambda_e = e_{33} / h_{33}$  and  $\Lambda_m = d_{33} / \gamma_{33}$ , respectively.

Next, the strip is subjected to an impact mechanical load with Heaviside time variation and the intensity  $\sigma_0 = 1 \text{ Pa}$ . The impermeable boundary conditions for the electric displacement and magnetic flux on the crack-faces are considered. The time variation of the normalized stress intensity factor is given in Fig. 7, where  $K_I^{stat} = 2.642 \text{ Pa} \cdot \text{m}^{1/2}$ . The boundary value problem for a homogeneous material has been analyzed also by the FEM code ANSYS. One can observe a quite good agreement of the results. For graded elasticity coefficients along the  $x_1$ -coordinate and a uniform mass density, the wave propagation is increasing with  $x_1$ . Therefore, the peak value of the SIF is reached in a shorter time instant in a functionally graded strip than that in a homogeneous one. The maximum value of the SIF is only slightly reduced for the cracked FGM strip.

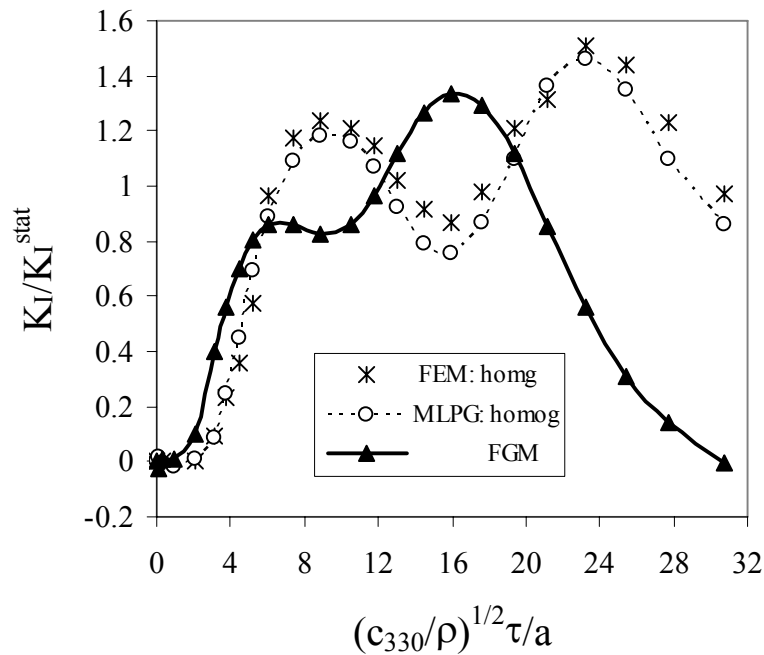


Fig. 7 Normalized stress intensity factor for an edge crack in a strip under a pure mechanical load  $\sigma_0 H(\tau - 0)$

#### 4. Conclusions

A meshless local Petrov-Galerkin method (MLPG) is presented for modelling of plane piezoelectric and magneto-electro-elastic problems. Both static and impact loads are considered. The Laplace-transform technique is applied to eliminate the time variable in the coupled governing partial differential equations. The analyzed domain is divided into small overlapping circular subdomains. A unit step function is used as the test function in the local weak-form of the governing partial differential equations. The derived local boundary-domain integral equations are non-singular. The moving least-squares (MLS) scheme is adopted for the approximation of the physical field quantities. The proposed method is a truly meshless method, which requires neither domain elements nor background cells in either the interpolation or the integration.

The present method is an alternative numerical tool to many existing computational methods such as the FEM or the BEM. The main advantage of the present method is its simplicity. Compared to the conventional BEM, the present method requires no fundamental solutions and all integrands in the present formulation are regular. Thus, no special numerical techniques are required to evaluate the integrals. It should be noted here that the fundamental solutions are not available for magneto-electro-elastic solids with continuously varying material properties in general cases. The present formulation also possesses the generality of the FEM. Therefore, the method is promising for numerical analysis of multi-field problems like piezoelectric, electro-magnetic or thermoelastic problems, which cannot be solved efficiently by the conventional BEM.

## 5. Acknowledgement

The authors acknowledge the support by the Slovak Science and Technology Assistance Agency registered under number APVV-0427-07, the Slovak Grant Agency VEGA-2/0039/09, and the German Research Foundation (DFG).

## 6. References

- Atluri, S.N. (2004) *The Meshless Method, (MLPG) For Domain & BIE Discretizations*. Tech Science Press, Forsyth.
- Atluri, S.N., Sladek, J., Sladek, V. & Zhu, T. (2000) The local boundary integral equation (LBIE) and its meshless implementation for linear elasticity. *Computational Mechanics*, 25, pp. 180-198.
- Atluri, S.N., Han, Z.D. & Shen, S. (2003) Meshless local Petrov-Galerkin (MLPG) approaches for solving the weakly-singular traction & displacement boundary integral equations. *CMES: Computer Modeling in Engineering & Sciences*, 4, pp. 507-516.
- Belytschko, T., Krogauz, Y., Organ, D., Fleming, M. & Krysl, P. (1996) Meshless methods; an overview and recent developments. *Comp. Meth. Appl. Mech. Engn.*, 139, pp. 3-47.
- Berlingcourt, D.A., Curran, D.R. & Jaffe, H. (1964): Piezoelectric and piezomagnetic materials and their function in transducers. *Physical Acoustics* 1, pp. 169-270.
- Dolbow, J.E. & Gosz, M. (2002) On computation of mixed-mode stress intensity factors in functionally graded materials. *Int. J. Solids Structures* 39, pp. 7065-7078.
- Eringen, C.E. & Maugin M.A. (1990) *Electrodynamics of Continua*. Springer-Verlag, Berlin.
- Feng, W.J. & Su, R.K.L. (2006) Dynamic internal crack problem of a functionally graded magneto-electro-elastic strip. *Int. J. Solids Structures* 43, pp. 5196-5216.
- Garcia-Sanchez, F., Saez, A. & Dominguez, J. (2005) Anisotropic and piezoelectric materials fracture analysis by BEM. *Computers & Structures*, 83, pp. 804-820.
- Garcia-Sanchez, F., Rojas-Diaz, R., Saez, A. & Zhang, Ch. (2007) Fracture of magneto-electroelastic composite materials using boundary element method (BEM). *Theoretical and Applied Fracture Mechanics* 47, pp. 192-204.
- Han, F., Pan, E., Roy, A.K. & Yue, Z.Q. (2006) Responses of piezoelectric, transversally isotropic, functionally graded and multilayered half spaces to uniform circular surface loading. *CMES: Computer Modeling in Engineering & Sciences*, 14, pp. 15-30.
- Landau, L.D. & Lifshitz, E.M. (1984) In: Lifshitz, E.M., Pitaevskii, L.P. (Eds.) *Electrodynamics of Continuous Media* (second edition). Pergamon Press, New York.
- Li, J.Y. (2000) Magneto-electroelastic multi-inclusion and inhomogeneity problems and their applications in composite materials. *International Journal of Engineering Science* 38, pp. 1993-2011.
- Liu, G.R., Dai, K.Y., Lim, K.M. & Gu, Y.T. (2002) A point interpolation mesh free method for static and frequency analysis of two-dimensional piezoelectric structures. *Computational Mechanics*, 29, pp. 510-519.
- Nan, C.W. (1994) Magneto-electric effect in composites of piezoelectric and piezomagnetic phases. *Phys. Rev. B*, 50, pp. 6082-6088.

- Ohs, R.R. & Aluru, N.R. (2001) Meshless analysis of piezoelectric devices. *Computational Mechanics*, 27, pp. 23-36.
- Parton, V.Z. & Kudryavtsev, B.A. (1988) *Electromagnetoelasticity, Piezoelectrics and Electrically Conductive Solids*. Gordon and Breach Science Publishers, New York.
- Parton, V.Z.; Kudryavtsev, B.A.; Senik, N.A. (1989) Electroelasticity. *Applied Mechanics: Soviet Review*, 2, pp. 1-58.
- Sladek, J., Sladek, V. & Atluri, S.N. (2000) Local boundary integral equation (LBIE) method for solving problems of elasticity with nonhomogeneous material properties. *Computational Mechanics*, 24, pp. 456-462.
- Sladek, J., Sladek, V. & Atluri, S.N. (2001) A pure contour formulation for meshless local boundary integral equation method in thermoelasticity, *CMES: Computer Modeling in Engr. & Sciences*, 2, pp. 423-434.
- Sladek, J., Sladek, V. & Van Keer, R. (2003) Meshless local boundary integral equation method for 2D elastodynamic problems. *Int. J. Num. Meth. Engr.*, 57, pp. 235-249.
- Sladek, J., Sladek, V. & Atluri, S.N. (2004) Meshless local Petrov-Galerkin method in anisotropic elasticity. *CMES: Computer Modeling in Engr. & Sciences*, 6, pp. 477-489.
- Sladek, J., Sladek, V., Zhang, Ch. Garcia-Sanchez, F. & Wünsche, M. (2006) Meshless local Petrov-Galerkin method for plane piezoelectricity. *CMC: Computers, Materials & Continua*, 4, pp. 109-118.
- Sladek, J., Sladek, V., Zhang, Ch., Solek, P. & Starek, L. (2007a) Fracture analyses in continuously nonhomogeneous piezoelectric solids by the MLPG. *CMES: Computer Modeling in Engr. & Sciences*, 19, pp. 247-262 .
- Sladek, J., Sladek, V., Zhang, Ch. & Solek, P. (2007b) Application of the MLPG to thermopiezoelectricity. *CMES: Computer Modeling in Engr. & Sciences*, 22, pp. 217–233.
- Suresh, S. & Mortensen A. (1998) *Fundamentals of Functionally Graded Materials*. Institute of Materials, London.
- Stehfest, H. (1970):Algorithm 368: numerical inversion of Laplace transform. *Comm. Assoc. Comput. Mach.*, 13, pp. 47-49.
- Wang, B.L. & Mai, Y.W. (2003) Crack tip field in piezoelectric/piezomagnetic media. *European Journal of Mechanics A/Solids* 22, pp. 591-602.
- Zhu, X., Wang, Z. & Meng, A. (1995) A functionally gradient piezoelectric actuator prepared by metallurgical process in PMN-PZ-PT system. *J. Mater. Sci Lett.*, 14, pp. 516-518.